Original Article

Magnoflorine attenuates Ang II-induced cardiac remodeling via promoting AMPK-regulated autophagy

Meili Zhu[1], Jiangbiao Hu[1], Yifan Pan[2], Qian Jiang[1], Chang Shu[3]

[1]Department of Rehabilitation Medicine, the First People's Hospital of Yongkang, Yongkang, China; [2]Department of Cardiology, the First People's Hospital of Yongkang, Yongkang, China; [3]Department of Medical, the First People's Hospital of Yongkang, Yongkang, China

Contributions: (I) Conception and design: C Shu, M Zhu; (II) Administrative support: J Hu; (III) Provision of study materials or patients: Y Pan; (IV) Collection and assembly of data: M Zhu, J Hu, Q Jiang; (V) Data analysis and interpretation: Y Pan, Q Jiang; (VI) Manuscript writing: All authors; (VII) Final approval of manuscript: All authors.

Correspondence to: Chang Shu, MM. Department of Medical, the First People's Hospital of Yongkang, 599 Jinshan West Road, Yongkang 321300, China. Email: shuchangsanbao@sina.com.

Background: Heart failure (HF) remains one of the most common events in the progression of hypertension. Magnoflorine (MNF) has been shown beneficial effects on the cardiovascular system. However, the action of MNF on angiotensin (Ang) II-induced cardiac remodeling and its underlying mechanisms have not yet been characterised. Here, we assessed the action of MNF in the development of hypertension-related HF.

Methods: C57BL/6 male mice were subjected to Ang II through a micro-osmotic pump infusion continuously for 4 weeks to induce hypertensive HF. MNF (10 and 20 mg/kg) was administered in the final 2 weeks. Ang II content was measured by enzyme-linked immunosorbent assay (ELISA) kit. Values of ejection fraction (EF) and fractional shortening (FS) were detected using an ultrasound diagnostic instrument. The mRNA levels of hypertrophic and fibrotic genes were determined by real-time quantitative polymerase chain reaction (RT-qPCR). Haematoxylin and eosin (H&E), wheat germ agglutinin (WGA), Masson trichrome, and Sirius Red staining were used to analyse pathologic changes in heart tissues. The expression levels of phosphorylated AMP-activated protein kinase (AMPK), light chain 3 microtubule associated protein II (LC3 II) to LC3 I, and p62 were detected by western blot assay.

Results: MNF significantly improved cardiac dysfunction and the content of creatine kinase-MB without altering blood pressure in Ang II-challenged mice. MNF obviously corrected the phenotypes of cardiac hypertrophy and fibrosis, including the high mRNA levels of atrial natriuretic peptide (*Anp*), brain natriuretic peptide (*Bnp*), collagen1a (*Col1a1*), transforming growth factor beta (*Tgfb1*), enlarged myocardial areas, and increased positive areas of Masson trichrome and Sirius Red staining. In addition, MNF alleviated oxidative injury, reflected by the upregulation of glutathione and the downregulation of reactive oxygen species and malondialdehyde. The activation of AMPK was elevated accompanied by an increased level of autophagy by MNF in hypertensive heart tissues. The therapeutic action of MNF was confirmed in Ang II-challenged H9c2 cells. Specifically, the AMPK inhibitor could eliminate the autophagy pathway in which MNF is involved.

Conclusions: MNF has benefits in hypertension-induced cardiac remodeling, which was partially associated with the improvement of oxidative stress via the mediation of the AMPK/autophagy axis.

Keywords: Hypertension; heart failure (HF); magnoflorine (MNF); autophagy; AMP-activated protein kinase (AMPK)

Submitted Mar 24, 2024. Accepted for publication Jun 27, 2024. Published online Aug 14, 2024.
doi: 10.21037/cdt-24-130
View this article at: https://dx.doi.org/10.21037/cdt-24-130

Introduction

Cardiac hypertrophy is now recognised as a leading cause of the clinical course of ventricular dilatation and heart failure (HF), which remains a determinant of mortality worldwide (1). This process mainly contributes to a variety of pathological stimuli, such as pressure overload, neurohormonal activation, myocardial ischemia, and hypoxia (2). Among these factors, angiotensin (Ang) II, a pivotal element of the renin-angiotensin system (RAS), plays a crucial role in the progress of cardiac remodeling characterised by left ventricular (LV) hypertrophy and cardiac fibrosis (3). Interestingly, Ang II also exerts non-haemodynamic effects, including cardiac autophagy, inflammation, and oxidative stress, which directly produce a harmful spike in the blood vessels and heart (4). It has reported that continuous infusion of Ang II in mice mimics patients with cardiac remodeling after pressure overload (5). Although experimental studies have demonstrated that the inhibition of RAS activity is associated with an improvement in HF (6), the identified mechanisms underlining hypertensive stress-mediated cardiac dysfunction remain a puzzle.

There is growing evidence to advocate for the important role of excessive autophagy and reactive oxygen species (ROS) in the pathophysiology of cardiac hypertrophy in both animal and human research (7,8). The light chain 3 microtubule associated protein (LC3), an important autophagy related protein, can be converted into LC3 I and subsequently become LC3 II, which is involved in the double membrane of the autophagosome (9). The scaffold protein p62 attracts ubiquitinated aggregates to the autophagosome and assists in their final degradation (9). Cardiac autophagy has been widely implicated in facilitating cell viability and heart function under stress (10). Studies have demonstrated that ROS production is associated with autophagy regulation. Cardiac hypertrophy results in elevated oxygen consumption, and excessive ROS leads to cardiac remodeling and failure (11). One of the upstream signaling elements of the autophagy process is AMP-activated protein kinase (AMPK), which acts as a central sensor in cells (12). When the cellular energy is low, elevated ROS and increased Ca^{2+} cause the phosphorylation of AMPK. Activated AMPK facilitates the regulation of autophagy in various myocardial diseases (13). Ang II stimulation inhibits AMPK activation in myocardial cells and affects cardiac hypertrophy and fibrosis (14). Therefore, the regulation of AMPK-mediated autophagy and oxidative stress may be a promising therapeutic strategy against cardiac damage. Magnoflorine (MNF) is a popular medicinal herb derived from Ziziphi Spinosae Semen, which is widely used in China for liver and heart dysfunction treatments (15). Recently, MNF has been shown to have various pharmacological activities. For example, pigs treated with MNF combined with hyaluronic acid-gel can promote subchondral bone regeneration in an osteoarthritis model (16). Notably, MNF has been found to regulates autophagy (Bcl-2/LC-3II) and oxidative stress in rats with type 2 diabetes mellitus (T2DM) (17). However, the role of MNF in Ang II-mediated cardiac injury has not been investigated.

In this study, we aimed to investigate whether MNF could protect against Ang II-mediated cardiac dysfunction in mice, and we explored the possible mechanisms of this process. We present this article in accordance with the ARRIVE reporting checklist (available at https://cdt.amegroups.com/article/view/10.21037/cdt-24-130/rc).

Highlight box

Key findings

- This study found that magnoflorine (MNF) treatment alleviated angiotensin (Ang) II-induced cardiac dysfunction, hypertrophy, and fibrosis in mice by suppression oxidative stress and promotion AMP-activated protein kinase (AMPK) activation and autophagy level. Furthermore, MNF improved Ang II-induced hypertrophy in cardiomyocytes via AMPK/autophagy axis.

What is known and what is new?

- Ang II could induce cardiac remodeling by suppression AMPK activation.
- MNF has benefits in hypertension-induced cardiac remodeling.

What is the implication, and what should change now?

- MNF is a potential therapeutic candidate for heart failure, and that AMPK/autophagy may be a promising target to ameliorate cardiac remodeling.

Methods

Animals

Male C57BL/6 mice (aged 6–8 weeks) were obtained from the Laboratory Animal Center of Zhejiang Province (Hangzhou, China). All mice were housed in a specific pathogen free (SPF) room at 22–25 ℃, with 45–65% humidity and a 12 h light-dark cycle. Mice were allowed free access to food and water. All mice were acclimation for 1 weeks before modeling. Experimental procedures were executed according to the National Institutes of Health

Guidelines for the Care and Use of Laboratory Animals. Animal care and experimental protocols were approved by the Ethics Committee of Laboratory Animal Care and Welfare, Zhejiang Academy Medical Sciences (approval No. 20200366).

Animal model

Total 28 C57BL/6 mice were randomly divided into four groups: (I) untreated mice as the control (Ctrl, n=7); (II) Ang II-infused mice as the model (Ang II, n=7); (III) Ang II-infused mice administration of a low-dose of MNF (Ang II + MNF 10 mg/kg, n=7); and (IV) Ang II-infused mice administration of a high-dose of MNF (Ang II + MNF 20 mg/kg, n=7). For grouping, we employ a random number table to perform randomization. Every mouse was assigned a temporary random number within the weight range. Ang II (cat. No. A107852, Aladdin, Shanghai, China) was dissolved in ddH_2O, infused into osmotic mini-pumps (cat. No. 1004, Alzet Model, CA, USA), implanted in subcutaneous, and delivered 1.44 mg/kg/day for four weeks. The control mice received equivalent ddH_2O through the osmotic mini-pumps. Systolic blood pressure was measured once a week using a non-invasive tail-cuff pressure analysis system (BP-98A, Softron, Tokyo, Japan). All mice with normal blood pressure (80–120 mmHg) were chosen to animal experiment. At 3th week, the systolic blood pressure <120 mmHg was eliminated, and all Ang II-infused mice reached the standard. MNF (Sigma-Aldrich, MO, USA) was dissolved in dimethyl sulfoxide (DMSO) as a stock solution stored in –80 ℃, and the MNF solution was diluted with normal saline and kept in a dark place. The mice were treated with MNF or normal saline once a day from the third week and continued for 2 weeks by gavage. The MNF dose was selected based on a previous study (18). All experimental procedures, including cage location, grouping, treatment, etc., were randomized to exclude potential influence. During animal experiment, there were no adverse events. Mice were anesthetised with phenobarbital sodium (40 mg/kg, i.p.) to reduce pain, and blood and heat tissues were harvested carefully. Serum was used to analyse creatine kinase-MB (CK-MB) using an automatic biochemical analyser (Beckman, California, USA).

Echocardiography

Mice were anesthetised with 2% isoflurane and placed in a supine position. Chest hair was removed with an electric shaver and commercial hair removal cream (Veet, London, UK). The LV internal diameter at end-diastole (LVIDs), LV end-diastolic diameters (LVIDd), interventricular septum thickness at diastole (IVSd), interventricular posterior wall thickness at diastole and systolic septal thickness were measured using an ultrasound diagnostic instrument (D6VET, VINNO, Jiangsu, China). The values of ejection fraction (EF) and fractional shortening (FS) were calculated using the following formula, respectively: EF% = [(end-systolic volumes – end-diastolic volumes) / end-systolic volumes]; FS% = [(LVIDd – LVIDs) / LVIDd].

Heart tissue staining

Heart tissues were collected, fixed in 4% paraformaldehyde and embedded in paraffin. The samples were incised into 5-μM thickness and stained with haematoxylin and eosin (H&E) to analyse pathologic changes. Wheat germ agglutinin (WGA) staining was used to analyse myocardial hypertrophy. Sirius Red staining was applied to detect collagen deposition, which Masson staining was applied to evaluate cardiac fibrosis. Three fields were randomly selected in each sample and were observed under an optical microscope (magnification: 200×, Leica Microsystems, Wetzlar, Germany). An observer who was blinded to the study performed pathological evaluations.

Real-time quantitative polymerase chain reaction (RT-qPCR)

Total RNA was purified from heart tissues and cells using TRIZOL reagent (19201ES60, Yeasen, Shanghai, China). Reverse transcription was achieved using Hifair® III 1st Strand cDNA Synthesis SuperMix (Yeasen). Quantitative PCR was carried out using Hieff UNICON® qPCR SYBR Green Master Mix (Yeasen) performed with the BioRad CFX96 TouchTM Real-Time PCR Detection System (Bio-Rad, Hercules, California, USA). Primers for atrial natriuretic peptide (*Anp*), brain natriuretic peptide (*Bnp*), collagen1a (*Col1a1*), transforming growth factor beta (*Tgfb1*), and *β-actin* were obtained from Sangon Biotech (Shanghai, China). Primer sequences are shown in *Table 1*. The relative amount of each gene was normalised to *β-actin*.

Cell culture and treatment

H9c2 cells were obtained from the Shanghai Institute of Biochemistry and Cell Biology (Shanghai, China), and

Table 1 Primers used for real-time quantitative polymerase chain reaction analysis

Gene	Species	Forward primer	Reverse primer
Anp	Mouse	5'-TACAGTGCGGTGTCCAACACAG-3'	5'-TGCTTCCTCAGTCTGCTCACTC-3'
Bnp	Mouse	5'-TCCTAGCCAGTCTCCAGAGCAA-3'	5'-GGTCCTTCAAGAGCTGTCTCTG-3'
Col1a1	Mouse	5'-TGGCCTTGGAGGAAACTTTG-3'	5'-CTTGGAAACCTTGTGGACCAG-3'
Tgfβ	Mouse	5'-TGACGTCACTGGAGTTGTACGG-3'	5'-GGTTCATGTCATGGATGGTGC-3'
β-actin	Mouse	5'-AGGCATTGTGATGGACTCCG-3'	5'-AGCTCAGTAACAGTCCGCCTA-3'

Anp, atrial natriuretic peptide; *Bnp*, brain natriuretic peptide; *Col1a1*, collagen1a; *Tgfb1*, transforming growth factor beta.

cultured in Duldecco's modified Eagle's medium (Biological Industries, Beit-Haemek, Israel) containing 10% foetal bovine serum (Every Green, Hangzhou, China) and 1% penicillin streptomycin solution (Bioship, Beijing, China). Cells were incubated at 37 ℃ with 5% CO_2. In cellular experiments, the H9c2 cells were stimulated with Ang II (1 μM) and treated with MNF for 48 h to measure the hypertrophic and fibrotic factors. MNF was dissolved in 1‰ DMSO, which was used as the vehicle control.

Assay of intracellular ROS, malondialdehyde (MDA) and glutathione (GSH)

The intracellular levels of ROS, MDA and GSH were measured using commercial assay kits (Beyotime Biotechnology, Jiangsu, China). Procedures were performed according to the manufacturer's instructions.

Western blotting

Heart tissues and cells were lysed with protein extraction buffer (Beyotime Biotechnology) containing a cocktail of protease and phosphatase inhibitor to extracted whole proteins. Protein concentration was quantified using a BCA reagent (Beyotime). Equal amounts of protein extracts were separated using SDS-polyacrylamide gel electrophoresis (EpiZyme, Shanghai, China), and then transferred to polyvinylidene fluoride membranes (Millipore, Darmstadt, Germany). After blocking with 5% non-fat milk (Servicebio, Wuhan, China) or 5% albumin bovine (Amresco, Washington, USA), the membranes were incubated with mouse anti-GAPDH (1:1,000, cat. No. 60004-1-Ig, Proteintech, Chicago, USA), rabbit anti-phospho-AMPKα (1:1,000, cat. No. 50081, CST, Boston, MA, USA), rabbit anti-AMPK (1:1,000, cat. No. 5832, CST), rabbit anti-LC3 (1:1,000, cat. No. 14600-1-IAP, Proteintech) and rabbit anti-p62 (1:1,000, cat. No. ab56416, Abcam, Cambridge, UK) at 4 ℃ overnight. After washing with Tris-buffered saline (TBS)-Tween buffer, the samples were incubated with horseradish peroxidase (HRP) labelled goat anti-mouse or goat anti-rabbit IgG (1:3,000, Servicebio) at room temperature for 2 h. The membranes were washed again with TBS-Tween buffer and visualised using an enhanced chemiluminescence kit (Servicebio). Band intensities were quantified using Image J software (NIH, Bethesda, MD, USA).

Statistical analysis

Sample sizes were defined by a priori power calculation with G-Power 3.1.9 software (http://www.gpower.hhu.de/). All data were collected and analyzed by two observers who were not aware of the group assignment or treatment of the animals. The data in each figure achieved normal distribution. All data were presented as mean ± standard deviation (SD), and the statistical analyses were performed using GraphPad Pro Prism 8.1 (GraphPad, CA, USA). The differences ($P<0.05$) were analysed with a one-way analysis of variance (ANOVA) followed by Tukey's multiple comparisons test.

Results

MNF attenuates Ang II-induced cardiac remodeling and dysfunction

To investigate whether MNF administration has a protective effect against cardiac injury, we established an Ang II-induced HF mouse model with a micro-osmotic pump for 4 weeks. The mice were treated with MNF at 10 and 20 mg/kg after 2 weeks of Ang II infusion. As expected, systolic blood pressure was significantly elevated after Ang II infusion, while MNF treatment did not reduce systolic

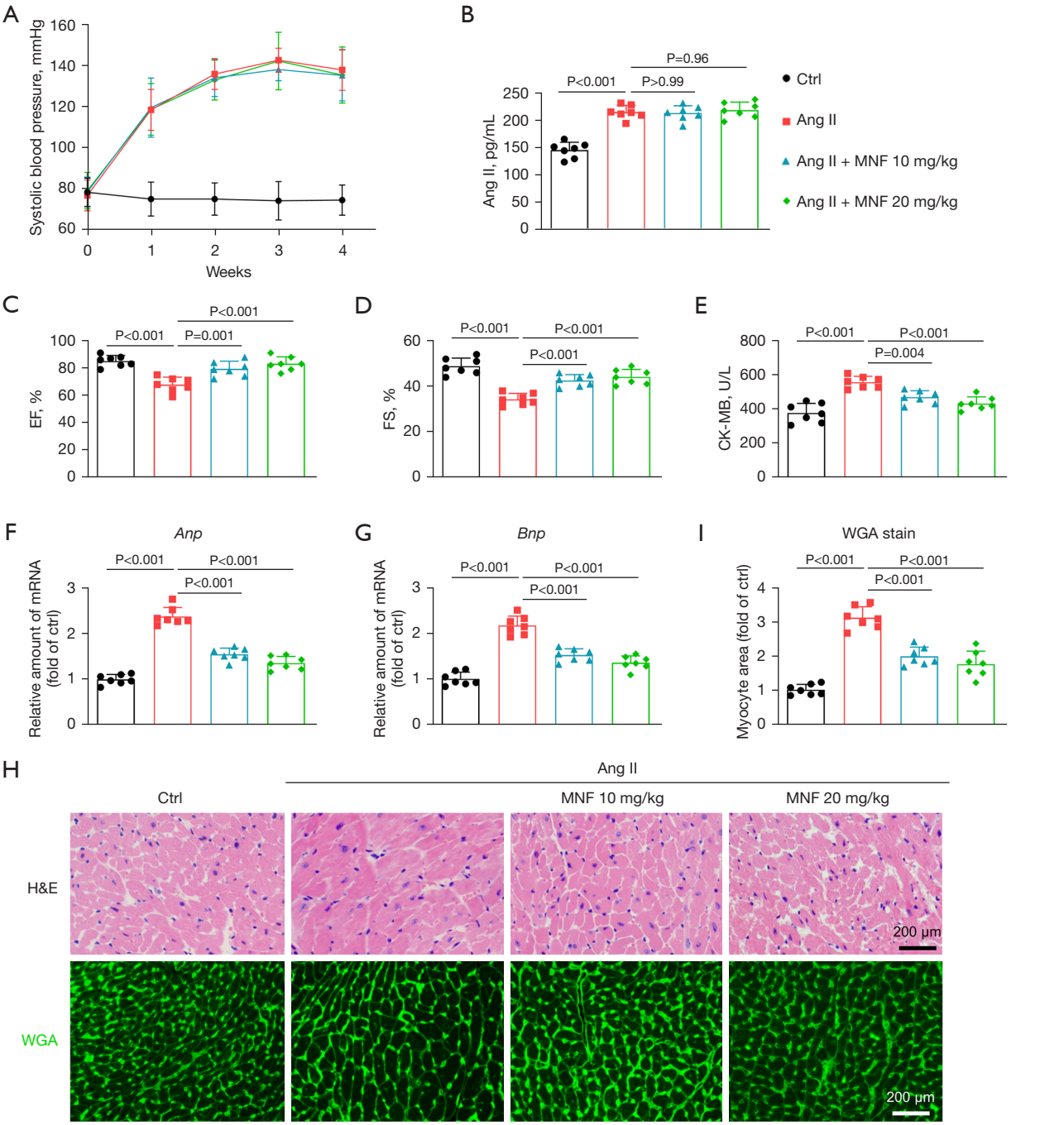

Figure 1 Effect of MNF on Ang II-induced cardiac remodeling and dysfunction in mice. The mice were treatment and groups as described in Methods section. (A) Systolic blood pressure of mice was measured every week. (B) Serum levels of Ang II was measured by ELISA assay. (C,D) Values of EF and FS were measured with an ultrasonic scanning image system. (E) The concentration of CK-MB was detected using a biochemical kit. (F,G) RT-qPCR was employed to analyze the mRNA levels of *Anp* and *Bnp* in heart tissues. (H) Representative images of H&E (upper lane) and WGA staining (lower lane) for mouse heart. (I) Quantitative analysis of cardiac area (n=7 per group). Data were presented as mean ± standard deviation. Ang II, angiotensin II; MNF, magnoflorine; RT-qPCR, real-time quantitative polymerase chain reaction; ELISA, enzyme-linked immunosorbent assay; EF, ejection fraction; FS, fractional shortening; CK-MB, creatine kinase-MB; H&E, hematoxylin-eosin; *Anp*, atrial natriuretic peptide; *Bnp*, brain natriuretic peptide; WGA, wheat germ agglutinin.

blood pressure in Ang II-challenged mice (*Figure 1A*). Ang II infusion also significantly increased by 71 pg/mL of Ang II in the serum (P<0.001), and no change was noted in mice treated with MNF (Ang II + MNF 10 mg/kg *vs.* Ang II: P>0.99; Ang II + MNF 20 mg/kg *vs.* Ang II: P=0.96; *Figure 1B*). Interestingly, non-invasive echocardiography examination showed that MNF improved by 11.57% (10 mg/kg) and 15.28% (20 mg/kg) of EF%, and 8.28% (10 mg/kg) and 9.85% (20 mg/kg) of FS% values in hypertensive mice (EF%: Ang II + MNF 10 mg/kg *vs.* Ang II: P=0.001, Ang II + MNF 20 mg/kg *vs.* Ang II: P<0.001; FS%: Ang II + MNF 10 mg/kg *vs.* Ang II: P<0.001, Ang II + MNF 20 mg/kg *vs.* Ang II: P<0.001; *Figure 1C,1D*). The increased level of CK-MB by Ang II infusion was also reduced by 88.2 and 124.6 U/L with 10 and 20 mg/kg MNF in serum, respectively (Ang II + MNF 10 mg/kg *vs.* Ang II: P=0.004; Ang II + MNF 20 mg/kg *vs.* Ang II: P<0.001; *Figure 1E*). In addition, MNF administration prevented elevated mRNA levels of *Anp* and *Bnp* in Ang II-challenged mice (*Anp*: Ang II + MNF 10 mg/kg *vs.* Ang II: P<0.001, Ang II + MNF 20 mg/kg *vs.* Ang II: P<0.001; *Bnp*: Ang II + MNF 10 mg/kg *vs.* Ang II: P<0.001, Ang II + MNF 20 mg/kg *vs*. Ang II: P<0.001; *Figure 1F,1G*). The pathological assessments were used to estimate cardiac morphological impairment. Both H&E and WGA staining of heart tissues showed hypertrophic changes in Ang II-challenged mice, and MNF clearly alleviated this pathological damage (WGA stain: Ang II + MNF 10 mg/kg *vs.* Ang II: P<0.001, Ang II + MNF 20 mg/kg *vs.* Ang II: P<0.001; *Figure 1H,1I*). These data suggest that MNF has protective effects on Ang II-induced cardiac hypertrophy and functional impairment in mice independent on antihypertensive effects.

MNF normalises Ang II-induced cardiac fibrosis and oxidative stress

We performed histological assessments and RT-qPCR of fibrosis and oxidative stress indexes in heart tissues to evaluate whether MNF is involved in protecting against cardiac fibrosis and oxidative stress. The transcript levels of *Col1a1* and *Tgfb1* were significantly elevated by 1.7 folds in heart tissues from the Ang II infusion group when compared to control mice (*Col1a1*: Ang II *vs.* Control: P<0.001; *Tgfb1*: Ang II *vs.* Control: P<0.001; *Figure 2A,2B*). Masson and Sirius Red staining exhibited increased fibrosis and interstitial collagen deposition in Ang II-challenged heart tissues (Masson stain: Ang II *vs.* Control: P<0.001; Sirius Red stain: Ang II *vs.* Control: P<0.001; *Figure 2C-2E*). MNF at 10 and 20 mg/kg normalised these Ang II-induced cardiac fibrosis (P<0.001, *Figure 2A-2E*). In addition, the level of GSH was significantly decreased in the Ang II infusion group compared with the control group (P<0.001, *Figure 2F*), and the levels of ROS and MDA were increased in Ang II-challenged heart tissues (P<0.001, *Figure 2G*). MNF was sufficient to reverse these antioxidative and oxidative parameters compared with the Ang II infusion group (P≤0.001, *Figure 2F,2G*). These results indicate that MNF plays a positive role in anti-fibrosis and anti-oxidative stress in the Ang II-induced HF mouse model.

Magnoflorine prevents Ang II-induced hypertrophy, fibrosis and oxidative stress in H9c2 cells

To confirm the study from our *in vivo* results, H9c2 cells stimulated with a 1 μM Ang II model were established *in vitro*. The transcript levels of *Anp*, *Bnp*, *Col1a1* and *Tgfb1* were significantly enhanced by 1.3, 1.0, 1.3, and 1.1 folds in the Ang II-induced H9c2 cells respectively (*Anp*: Ang II *vs.* Control: P<0.001; *Bnp*: Ang II *vs.* Control: P<0.001; *Col1a1*: Ang II *vs.* Control: P<0.001; *Tgfb1*: Ang II *vs.* Control: P<0.001; *Figure 3A,3B*), while MNF at 10 and 20 μM obviously reduced the hypertrophic and fibrotic factors (*Anp*: Ang II + MNF 10 mg/kg *vs.* Ang II: P<0.001, Ang II + MNF 20 mg/kg *vs.* Ang II: P<0.001; *Bnp*: Ang II + MNF 10 mg/kg *vs.* Ang II: P<0.001, Ang II + MNF 20 mg/kg *vs.* Ang II: P<0.001; *Col1a1*: Ang II + MNF 10 mg/kg *vs.* Ang II: P<0.001, Ang II + MNF 20 mg/kg *vs.* Ang II: P<0.001; *Tgfb1*: Ang II + MNF 10 mg/kg *vs.* Ang II: P<0.001, Ang II + MNF 20 mg/kg *vs.* Ang II: P<0.001; *Figure 3A,3B*). The concentration of GSH was significantly lower in Ang II-induced H9c2 cells than in the control group (P=0.004, *Figure 3C*). MNF treatment reversed the GSH content compared with the Ang II-induced H9c2 cells (Ang II + MNF 10 mg/kg *vs.* Ang II: P=0.041; Ang II + MNF 20 mg/kg *vs.* Ang II: P=0.007; *Figure 3C*). In addition, MNF decreased by 1.53 folds (10 μM) and 1.81 folds (20 μM) of ROS level, and 1.55 folds (10 μM) and 2.11 folds (20 μM) of MDA compared with the Ang II-induced H9c2 cells (P<0.001, *Figure 3D*).

Magnoflorine protects cardiomyocytes via the AMPK-mediated autophagy

To investigate the molecular mechanist insights into

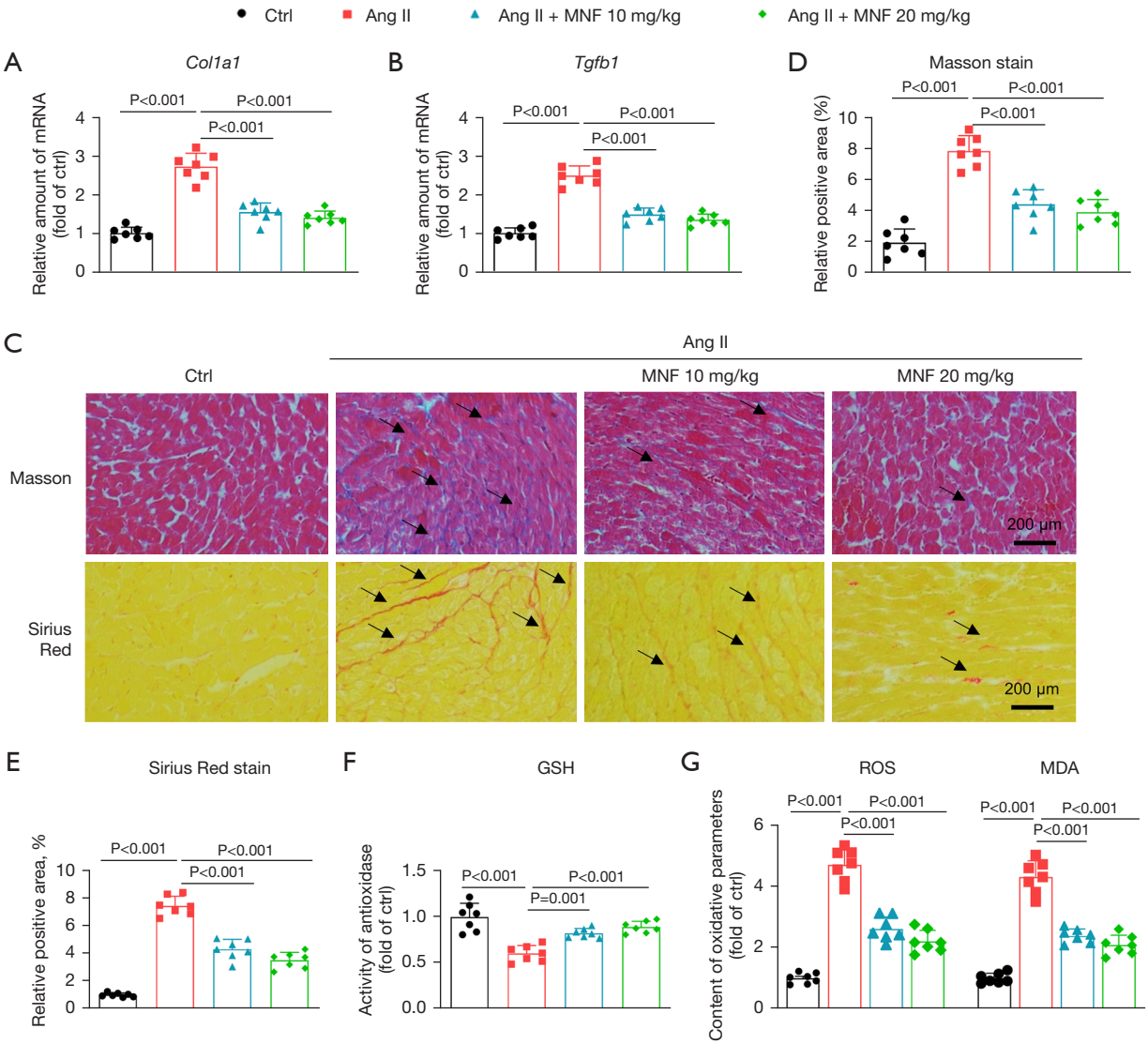

Figure 2 Effect of MNF on Ang II-induced hypertrophy, fibrosis and oxidative stress in mice. (A,B) MNF treatment significantly decreased the Ang II-induced elevation of mRNA levels of *Col1a1* and *Tgfb1* in heart tissues. (C) Representative images of Masson staining (upper lane) and Sirius Red staining (lower lane) for mouse heart. Black arrows indicate positive staining. (D,E) Quantitative analysis of fibrotic areas from Masson staining or Sirius Red staining. (F,G) The concentrations of GSH, ROS, and MDA in heart tissues were detected (n=7 per group). Data were presented as mean ± standard deviation. Ang II, angiotensin II; MNF, magnoflorine; GSH, glutathione; ROS, reactive oxygen species; MDA, malondialdehyde; *Col1a1*, collagen1a; *Tgfb1*, transforming growth factor beta.

the efficiency of MNF in Ang II-induced myocardial damage, we determined the protein levels of AMPK and autophagy-related proteins in heart tissues and H9c2 cells. MNF treatment significantly alleviated the Ang II-induced inhibition of AMPK activation and autophagy level, as evidenced by the upregulation by 0.26 folds of p-AMPK to AMPK ratio and 0.33 folds LC3 II to LC3 I and the downregulation by 0.59 folds of p62 protein in the Ang II-induced H9c2 cells (p-AMPK/AMPK: Ang II + MNF 20 μM *vs.* Ang II: P=0.01; LC3 II /LC3 I: Ang II + MNF 20 μM *vs.* Ang II: P=0.02; p62: Ang II + MNF 20 μM *vs.* Ang II: P=0.001; *Figure 3E*). Similarly, phosphorylation of AMPK and LC3 II to LC3 I were significantly increased by 0.33 folds (p-AMPK/AMPK) and 0.56 folds (LC3 II/LC3 I), and

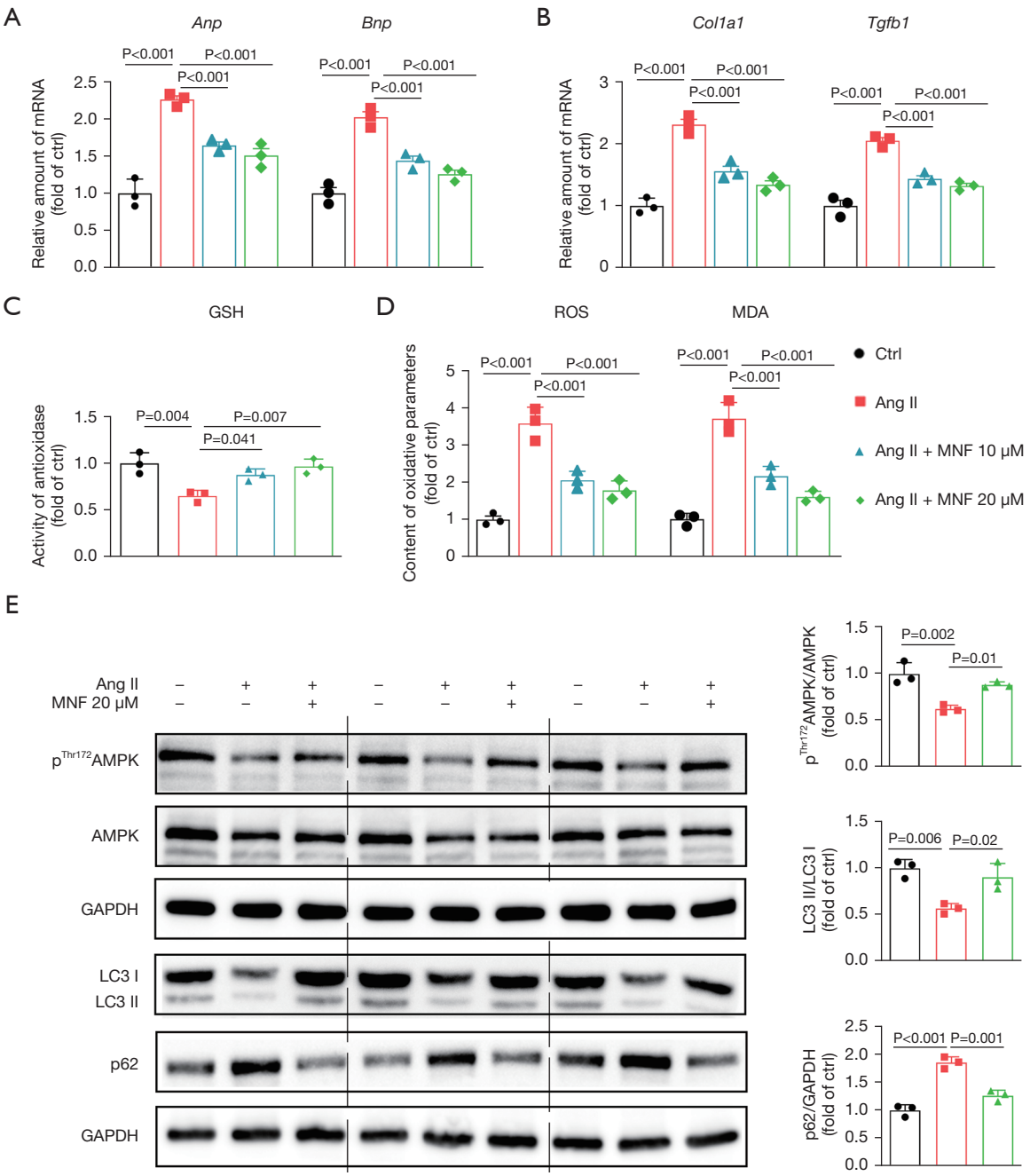

Figure 3 Effect of MNF on Ang II-induced myocardial damage and the activation of AMPK and autophagy in H9c2 cells. H9c2 cells were treated with MNF (10 and 20 μM) for 30 min and then stimulated with Ang II (1 μM) and MNF for 24 h. The control group treated with equal volume vehicle. (A,B) MNF treatment significantly decreased the mRNA levels of *Anp*, *Bnp*, *Col1a1* and *Tgfb1* in Ang II-induced H9c2 cells. (C,D) The levels of GSH, ROS, and MDA were measured in Ang II-induced H9c2 cells. (E) Western blot was used to evaluate the protein expression levels of p-AMPK, AMPK, LC3 II to LC3 I, and p62 in H9c2 cells (n=3 per group). Data were presented as mean ± standard deviation. Ang II, angiotensin II; MNF, magnoflorine; AMPK, AMP-activated protein kinase; LC3, light chain 3 microtubule associated protein; GSH, glutathione; ROS, reactive oxygen species; MDA, malondialdehyde; *Anp*, atrial natriuretic peptide; *Bnp*, brain natriuretic peptide; *Col1a1*, collagen1a; *Tgfb1*, transforming growth factor beta.

p62 level were decreased by 0.33 folds with MNF treatment in the Ang II infusion group (p-AMPK/AMPK: Ang II + MNF 20 mg/kg *vs.* Ang II: P=0.008; LC3 II/LC3 I: Ang II + MNF 20 mg/kg *vs.* Ang II: P=0.01; p62: Ang II + MNF 20 mg/kg *vs.* Ang II: P<0.001; *Figure 4A*).

To clarify whether autophagy-mediated cardiac damage was dependent on the inactivation of AMPK, we used an AMPK inhibitor, compound C, to pretreat the H9c2 cells for 30 min before MNF treatment. MNF enhanced the autophagy activation in the Ang II-challenged H9c2 cells (P≤0.001, *Figure 4B*), while compound C did not eliminate these enhancements (LC3 II/LC3 I: Ang II + MNF + CC *vs.* Ang II + MNF: P=0.009; p62: Ang II + MNF + CC *vs.* Ang II + MNF: P<0.001; *Figure 4B*). These data provide evidence that MNF protects against Ang II-induced hypertrophy, fibrosis and oxidative stress via promoting AMPK-regulated autophagy activation.

Discussion

In the current study, we showed the efficacy of MNF in improving cardiac injury and its underlying mechanisms in the context of hypertension. We found that MNF treatment corrected deficiencies, such as cardiac dysfunction, hypertrophy, and fibrosis in an Ang II-induced HF mouse model. In addition, Ang II activated oxidative stress, and suppressed AMPK activation and the autophagy level in mouse heart tissues and cultured cardiomyocytes, which were significantly reversed by MNF. Notably, AMPK inhibition by a small molecule compound blocked the innately pharmacological effects of MNF on H9c2 cells. The results indicate that MNF is a potential therapeutic candidate for HF, and that AMPK/autophagy may be a promising target to ameliorate cardiac remodeling (*Figure 5*).

This study has a notable limitation. There were 7 mice in each group, the sample size is small and may cause bias. Thus, these results are necessary to be verified in a large number of samples in the future.

Hypertensive cardiac remodeling is commonly characterised by cardiac hypertrophy and fibrosis, which may cause HF and even sudden death (19,20). Clinical trials have shown that the management of controlling blood pressure cannot effectively reverse cardiac remodeling under the pathologic condition of hypertension (21). Therapies targeting hypertension-related cardiac remodeling is limited. Therefore, pharmacological candidates are extraordinarily needed for HF treatment. Recent research has demonstrated that several kinds of native compounds, such as diacerein (22), celastrol (23) and leonurine (24), could prevent the development of cardiac injury and dysfunction by alleviating inflammation in a hypertension mouse model. Natural products may be a candidate bank for agent discovery of hypertension-related heart disorders. MNF has been demonstrated to possess several pharmacological activities, including anti-inflammation, anti-oxidant, and treatment of metabolic disorders (18,25,26). MNF partially protects against a lipopolysaccharide-induced inflammation response in an acute lung injury model partially via suppressing Toll-like receptor 4-mediated NF-κB and MAPK pathways (25). A recent study has reported that MNF could contribute to reduction of the fasting blood glucose level and prevent skeletal muscle atrophy in T2DM rats (17). However, there are barely any studies on hypertensive mice exploring the therapeutic action of MNF in cardiac remodeling. In this study, cardiac hypertrophy, fibrosis and dysfunction were observed in Ang II-induced hypertensive mice. Notably, we found that MNF, as a natural compound, could significantly ameliorate the above undesirable symptoms, without affecting blood pressure.

Autophagy has been reported to be closely connected with the progression of cardiac remodeling (27-30). Growing evidence indicates that autophagy regarded as a conserved process that contributes to maintaining cell and tissue homeostasis under normal or stress conditions, including changes in metabolism, energy and oxygen status (31). The role of autophagy in mediating cardiac function under Ang II-stimulated conditions seems complicated. Some studies have shown that excessive autophagy in myocardial contributes to the progress of hypertrophy and HF (27,28). Conversely, other studies have reported that autophagy exhibits beneficial effects on myocardial cells in failing hearts either from pressure overload or isoproterenol induction (29,31). In addition, MNF has been found to effectively downregulate the expression of autophagy (Bcl-2/LC3B) in T2DM rats (17). However, in the present study, we found that Ang II inhibited autophagy, as reflected by the decreased ratio of LC3 II to LC3 I and the increased level of p62 in mouse heart tissues and cultured cardiomyocytes, which were remarkedly reversed by the treatment with MNF. This paradoxical phenomenon may be attributed to differences in animal models and pathological conditions.

The modulation and associated mechanisms of cardiac autophagy remain unclear. Oxidative stress has been shown to play a pivotal role in the autophagy regulation. Cardiac hypertrophy results in elevated oxygen consumption, thus producing excessive ROS (32). ROS modulates autophagy

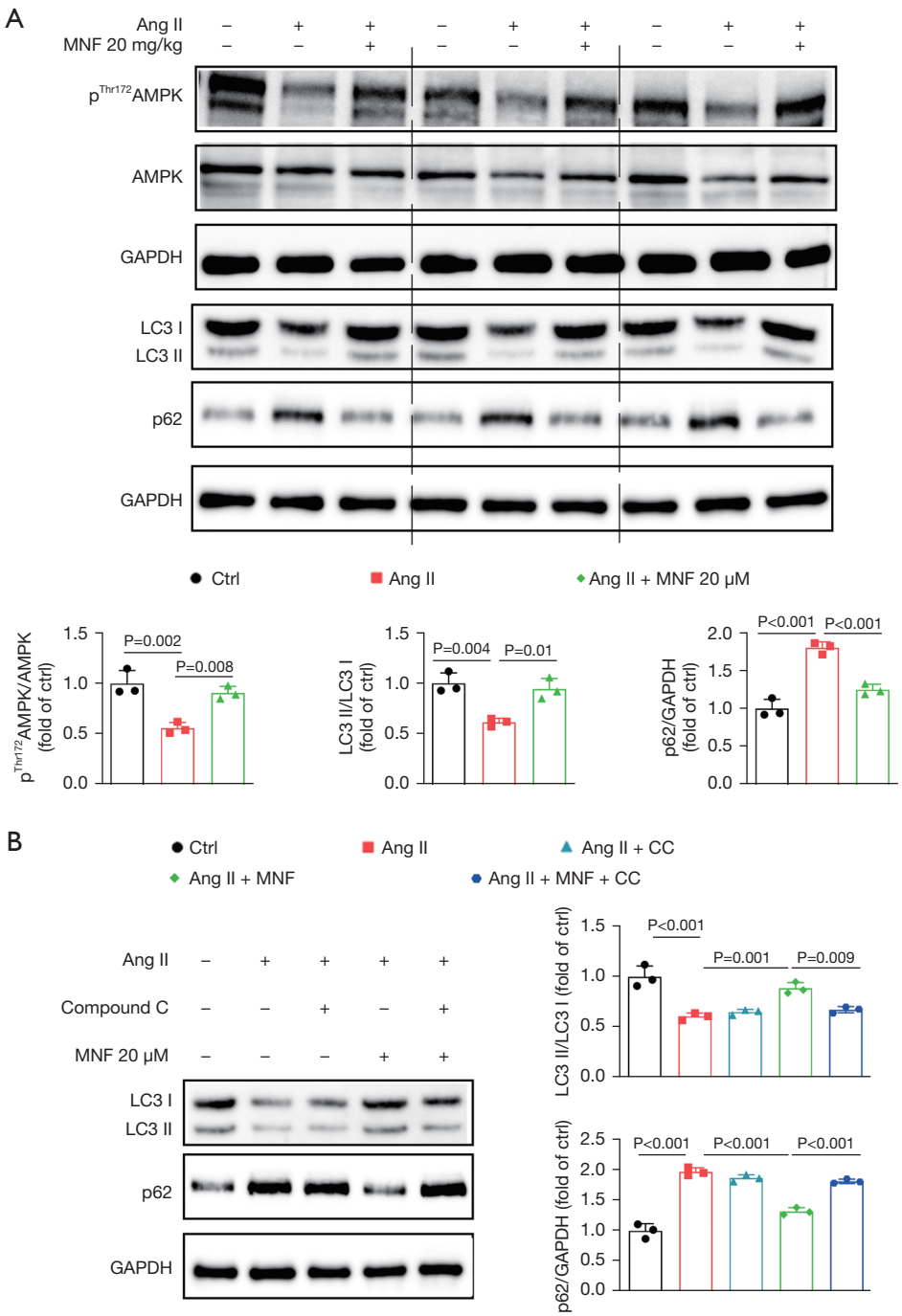

Figure 4 MNF protects cardiomyocytes via the AMPK-mediated autophagy activation. (A) MNF administration significantly upregulated the expression levels of p-AMPK to AMPK and p62, and downregulated the ratio of LC3 II to LC3 I in Ang II-induced heart tissues. H9c2 cells were pretreated with CC for 30 min and then co-incubation with Ang II, CC and MNF for 6 h. (B) Western blot was applied for evaluation the protein expression levels of LC3 II to LC3 I and p62 (n=3 per group). Data were presented as mean ± standard deviation. Ang II, angiotensin II; MNF, magnoflorine; AMPK, AMP-activated protein kinase; LC3, light chain 3 microtubule associated protein; CC, compound C.

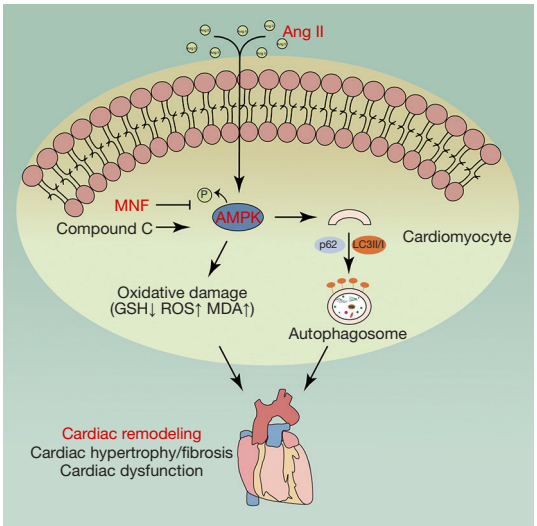

Figure 5 Schematic overview of the protective effect of MNF on cardiac remodeling via AMPK/autophagy axis in cardiomyocytes. Ang II, angiotensin II; AMPK, AMP-activated protein kinase; MNF, magnoflorine; GSH, glutathione; ROS, reactive oxygen species; MDA, malondialdehyde; LC3, light chain 3 microtubule associated protein.

via various mechanisms including catalase, Atg4 and the mitochondrial electron transport chains (33). In this study, MNF significantly attenuated Ang II-induced oxidative stress, manifested as the upregulation the level of GSH and downregulation of ROS and MDA in cardiac tissue and cells.

AMPK, a key moderator for maintaining energy balance, is part of one of the important upstream signaling pathways of autophagy in various tissues, such as the endothelium, liver and heart (34). Abnormal AMPK activation involves the pathogenesis of cardiac hypertrophy, fibrosis and remodeling via affecting cellular metabolism (35). AMPK activity is commonly positively associated with autophagy levels under cardiac damage conditions. Activation of AMPK results in increased autophagy in Ang II-induced heart tissues (36). It should be noted that MNF could elevate the cerebral ischemia-induced inactivation of AMPK in the cortex of rats (18). Consistent with this result, our data showed that MNF significantly upregulated phosphorylated AMPK both in cardiac tissues and H9c2 cells challenged with Ang II. Moreover, the inhibition of AMPK could eliminate the regulation effect of MNF on autophagy in H9c2 cells. Findings from the current study demonstrated that MNF protects against cardiac remodeling in hypertensive mice in association with the regulation of the AMPK/autophagy pathway.

Conclusions

In summary, this study demonstrates the pharmacological effects of MNF on Ang II-challenged mice and reveals that the modulation of the AMPK/autophagy pathway by MNF contributes to the amelioration of cardiac hypertrophy, fibrosis and dysfunction. Therefore, the regulation of the AMPK/autophagy axis of MNF may be a potential target for the treatment of hypertensive-related HF.

Acknowledgments

Funding: The study was supported by the Biological Medicine and Health Industry Development Support Science and Technology Project of Hangzhou (Nos. 2022WJC050 and 2022WJC049), and the Zhejiang TCM Scientific Research Foundation (No. 2022ZB083).

Footnote

Reporting Checklist: The authors have completed the ARRIVE reporting checklist. Available at https://cdt.amegroups.com/article/view/10.21037/cdt-24-130/rc

Data Sharing Statement: Available at https://cdt.amegroups.com/article/view/10.21037/cdt-24-130/dss

Peer Review File: Available at https://cdt.amegroups.com/article/view/10.21037/cdt-24-130/prf

Conflicts of Interest: All authors have completed the ICMJE uniform disclosure form (available at https://cdt.amegroups.com/article/view/10.21037/cdt-24-130/coif). All authors report that this study was supported by the Biological Medicine and Health Industry Development Support Science and Technology Project of Hangzhou (Nos. 2022WJC050 and 2022WJC049), and the Zhejiang TCM Scientific Research Foundation (No. 2022ZB083). The authors have no other conflicts of interest to declare.

Ethical Statement: The authors are accountable for all aspects of the work in ensuring that questions related to the accuracy or integrity of any part of the work are appropriately investigated and resolved. Experimental procedures were executed according to the National Institutes of Health Guidelines for the Care and Use of Laboratory Animals. Animal care and experimental protocols were approved by the Ethics Committee of Laboratory Animal Care and Welfare, Zhejiang Academy

Medical Sciences (approval No. 20200366).

References

1. Ritterhoff J, Tian R. Metabolic mechanisms in physiological and pathological cardiac hypertrophy: new paradigms and challenges. Nat Rev Cardiol 2023;20:812-29.
2. Bazgir F, Nau J, Nakhaei-Rad S, et al. The Microenvironment of the Pathogenesis of Cardiac Hypertrophy. Cells 2023;12:1780.
3. Shi J, Yang C, Zhang J, et al. NAT10 Is Involved in Cardiac Remodeling Through ac4C-Mediated Transcriptomic Regulation. Circ Res 2023;133:989-1002.
4. Yu T, Xu X, Wei J, et al. Ginsenoside Rg5 alleviates Ang II-induced cardiac inflammation and remodeling by inhibiting the JNK/AP-1 pathway. Int Immunopharmacol 2023;120:110408.
5. McCaffrey SL, Lim G, Bullock M, et al. The Histamine 3 Receptor Is Expressed in the Heart and Its Activation Opposes Adverse Cardiac Remodeling in the Angiotensin II Mouse Model. Int J Mol Sci 2020;21:9757.
6. Hedayati N, Yaghoobi A, Salami M, et al. Impact of polyphenols on heart failure and cardiac hypertrophy: clinical effects and molecular mechanisms. Front Cardiovasc Med 2023;10:1174816.
7. Liu H, Zhou Z, Deng H, et al. Trim65 attenuates isoproterenol-induced cardiac hypertrophy by promoting autophagy and ameliorating mitochondrial dysfunction via the Jak1/Stat1 signaling pathway. Eur J Pharmacol 2023;949:175735.
8. Luo F, Fu M, Wang T, et al. Down-regulation of the mitochondrial fusion protein Opa1/Mfn2 promotes cardiomyocyte hypertrophy in Su5416/hypoxia-induced pulmonary hypertension rats. Arch Biochem Biophys 2023;747:109743.
9. Li X, He S, Ma B. Autophagy and autophagy-related proteins in cancer. Mol Cancer 2020;19:12.
10. Wu X, Liu Z, Yu XY, et al. Autophagy and cardiac diseases: Therapeutic potential of natural products. Med Res Rev 2021;41:314-41.
11. Wang F, Liang Q, Ma Y, et al. Silica nanoparticles induce pyroptosis and cardiac hypertrophy via ROS/NLRP3/Caspase-1 pathway. Free Radic Biol Med 2022;182:171-81.
12. Cui YK, Hong YX, Wu WY, et al. Acacetin ameliorates cardiac hypertrophy by activating Sirt1/AMPK/PGC-1α pathway. Eur J Pharmacol 2022;920:174858.
13. Lu QB, Ding Y, Liu Y, et al. Metrnl ameliorates diabetic cardiomyopathy via inactivation of cGAS/STING signaling dependent on LKB1/AMPK/ULK1-mediated autophagy. J Adv Res 2023;51:161-79.
14. Xu M, Xue RQ, Lu Y, et al. Choline ameliorates cardiac hypertrophy by regulating metabolic remodelling and UPRmt through SIRT3-AMPK pathway. Cardiovasc Res 2019;115:530-45.
15. Okon E, Kukula-Koch W, Jarzab A, et al. Advances in Chemistry and Bioactivity of Magnoflorine and Magnoflorine-Containing Extracts. Int J Mol Sci 2020;21:1330.
16. Cai Z, Feng Y, Li C, et al. Magnoflorine with hyaluronic acid gel promotes subchondral bone regeneration and attenuates cartilage degeneration in early osteoarthritis. Bone 2018;116:266-78.
17. Yadav A, Singh A, Phogat J, et al. Magnoflorine prevent the skeletal muscle atrophy via Akt/mTOR/FoxO signal pathway and increase slow-MyHC production in streptozotocin-induced diabetic rats. J Ethnopharmacol 2021;267:113510.
18. Liang H, Chang X, Xia R, et al. Magnoflorine Attenuates Cerebral Ischemia-Induced Neuronal Injury via Autophagy/Sirt1/AMPK Signaling Pathway. Evid Based Complement Alternat Med 2022;2022:2131561.
19. Stanko P, Repova K, Baka T, et al. Sacubitril/Valsartan Alleviates Cardiac Remodeling and Dysfunction in L-NAME-Induced Hypertension and Hypertensive Heart Disease. Biomedicines 2024;12:733.
20. Eghan P, Folson AA, Donkor A, et al. Relationship between hypertensive disorders of pregnancy (HDP) and cardiac remodeling during pregnancy: Systematic review and meta-analysis. Eur J Obstet Gynecol Reprod Biol 2024;298:108-15.
21. Di Palo KE, Barone NJ. Hypertension and Heart Failure: Prevention, Targets, and Treatment. Cardiol Clin 2022;40:237-44.
22. Wang M, Luo W, Yu T, et al. Diacerein alleviates Ang II-induced cardiac inflammation and remodeling by inhibiting the MAPKs/c-Myc pathway. Phytomedicine

2022;106:154387.
23. Ye S, Luo W, Khan ZA, et al. Celastrol Attenuates Angiotensin II-Induced Cardiac Remodeling by Targeting STAT3. Circ Res 2020;126:1007-23.
24. Shen S, Wu G, Luo W, et al. Leonurine attenuates angiotensin II-induced cardiac injury and dysfunction via inhibiting MAPK and NF-κB pathway. Phytomedicine 2023;108:154519.
25. Guo S, Jiang K, Wu H, et al. Magnoflorine Ameliorates Lipopolysaccharide-Induced Acute Lung Injury via Suppressing NF-κB and MAPK Activation. Front Pharmacol 2018;9:982.
26. Xu T, Kuang T, Du H, et al. Magnoflorine: A review of its pharmacology, pharmacokinetics and toxicity. Pharmacol Res 2020;152:104632.
27. Gil-Cayuela C, López A, Martínez-Dolz L, et al. The altered expression of autophagy-related genes participates in heart failure: NRBP2 and CALCOCO2 are associated with left ventricular dysfunction parameters in human dilated cardiomyopathy. PLoS One 2019;14:e0215818.
28. Guo X, Zhang Y, Lu C, et al. Protective effect of hyperoside on heart failure rats via attenuating myocardial apoptosis and inducing autophagy. Biosci Biotechnol Biochem 2020;84:714-24.
29. Oyabu J, Yamaguchi O, Hikoso S, et al. Autophagy-mediated degradation is necessary for regression of cardiac hypertrophy during ventricular unloading. Biochem Biophys Res Commun 2013;441:787-92.
30. Nakai A, Yamaguchi O, Takeda T, et al. The role of autophagy in cardiomyocytes in the basal state and in response to hemodynamic stress. Nat Med 2007;13:619-24.
31. Ichimiya T, Yamakawa T, Hirano T, et al. Autophagy and Autophagy-Related Diseases: A Review. Int J Mol Sci 2020;21:8974.
32. Liu X, Zhang W, Luo J, et al. TRIM21 deficiency protects against atrial inflammation and remodeling post myocardial infarction by attenuating oxidative stress. Redox Biol 2023;62:102679.
33. Niu C, Jiang D, Guo Y, et al. Spermidine suppresses oxidative stress and ferroptosis by Nrf2/HO-1/GPX4 and Akt/FHC/ACSL4 pathway to alleviate ovarian damage. Life Sci 2023;332:122109.
34. Gao Y, Zhao D, Xie WZ, et al. Rap1GAP Mediates Angiotensin II-Induced Cardiomyocyte Hypertrophy by Inhibiting Autophagy and Increasing Oxidative Stress. Oxid Med Cell Longev 2021;2021:7848027.
35. Feng Y, Zhang Y, Xiao H. AMPK and cardiac remodelling. Sci China Life Sci 2018;61:14-23.
36. Liu J, Li X, Lu Q, et al. AMPK: a balancer of the renin-angiotensin system. Biosci Rep 2019;39:BSR20181994.

Cite this article as: Zhu M, Hu J, Pan Y, Jiang Q, Shu C. Magnoflorine attenuates Ang II-induced cardiac remodeling via promoting AMPK-regulated autophagy. Cardiovasc Diagn Ther 2024;14(4):576-588. doi: 10.21037/cdt-24-130

